

# Performance Analysis and Comparison of Non-Inverting Buck-Boost Converter Using PI, OCC, and Hybrid OCC-PI Control

Ahmet Karaarslan, Ali Shaibu\*

Electrical and Electronic Engineering, Ankara Yildirim Beyazit University, Turkey

\*Corresponding author, email: shaibu.ali.imran@gmail.com

---

**Abstract** – *The study compares and analyses the performance of the one-cycle control (OCC), hybrid one-cycle-proportional integral control (OCC-PI), and the conventional PI control method applied to the non-inverting buck-boost converter. The hybrid OCC-PI control method combines the OCC and PI control techniques to provide a hybrid non-linear closed-loop control technique for regulating the buck-boost converter. The MATLAB/Simulink equivalent system model was simulated with design parameter variations using a wide input voltage range of 9 – 36 V, a nominal output voltage of 28 V, and a fixed switching frequency of 250 kHz to validate the control response speed, reliability, and robustness of the proposed control technique. The simulation results due to input voltage, output voltage, and load variations were carried out while recording the settling time, overshoots, efficiency, output voltage, and inductor current ripples due to each applied control technique. The simulation results indicated that the Hybrid OCC-PI control provides better response speed and a lower output voltage overshoot relative to the PI. It also provides better reference voltage tracking compared to the OCC control method.*

**Keywords:** *One-Cycle Control, DC-DC Converter, Buck-Boost Converter, Hybrid OCC-PI*

---

## I. Introduction

Switched Mode Power Supply (SMPS) have become an integral aspect of most industrial, military, domestic electronic equipment as well as in renewable energy generation methods, hence increasing research interest on the topic to provide further insight into efficient converter topologies and highly effective control methods for such converters [1-4]. The switching converters unlike the linear regulators, convert Direct Current (DC) voltage from one voltage level to another as per the required input characteristic of the load.

Converter topologies are classified as isolated or non-isolated depending on the presence of an isolation transformer between the input and the load or not, as such, the commonly employed converters include the buck, boost, buck-boost, SEPIC, Cuk, flyback, full-bridge etc. [5,6]. The conversion of voltage is achieved by momentarily storing the input energy in the magnetic and electric field of inductors

and capacitors respectively, which is subsequently released to the load [7-9]. The amount of energy transferred from the input to output is dependent on the applied frequency and duty cycle to a particular DC-DC converter topology, hence the input current, output current, output voltage and power can be controlled effectively.

Because of the growing research interest in power electronics control methods as a result of the wide range of converter applications, various improvements in control techniques for DC-DC converters, such as model predictive [10,11], sliding mode, hysteresis [12], fuzzy logic [13], and linear control methodologies, are presented in the literature for the optimal control of converters. The PI control is the widely used control method for DC-DC converter due to the simplicity of implementation, however, it presents poor dynamic response due to the non-linearity of switching converters consequently negatively affecting the robustness of the converter [14]. The one-cycle control (OCC) method is a non-linear control technique that

employs the concept of averaging value of the switching variable for each cycle [15]. In [16] used the OCC control approach to regulate an isolated flyback converter for proton exchange membrane (PEM) fuel cells, whilst [17] used one cycle control of the non-inverting buck-boost converter. The one-cycle control approach, as applied to various DC-DC converter topologies, was given in [17-21] as a non-linear control strategy for effective converter control, as opposed to linear control methods such as the PI control method. The results show that OCC control outperforms PI control approaches in terms of faster dynamic response and reduced overshoots when system parameters are varied. The main closed-loop control of the OCC did not include the output voltage, but it did contain the input voltage and constant reference voltage, preventing a full closed-loop from being achieved. In [20], a modified OCC control method applied to a SEPIC converter was presented as a more robust alternative to the conventional OCC control technique by incorporating the output voltage in the control loop; the results show a significant improvement in dynamic response however, higher output voltage perturbation due to load variation was observed.

The objective of this research is to investigate the performance and operation of the hybrid OCC-PI controlled non-inverting buck-boost converter topology, which has a wide input and output voltage range and relatively low voltage stress on switching devices. By comparing the response characteristics of the proportional-integral (PI) control, One Cycle Control (OCC) and the Hybrid One Cycle Control-PI (OCC-PI) approach, the performance and robustness of the applied control methods are also analysed.

## II. Converter Topology

The non-inverting buck-boost converter topology is realized by the amalgamation and simplification of the cascaded buck and boost converters as depicted in Fig 1 showing the single-leg two switch buck-boost converter.

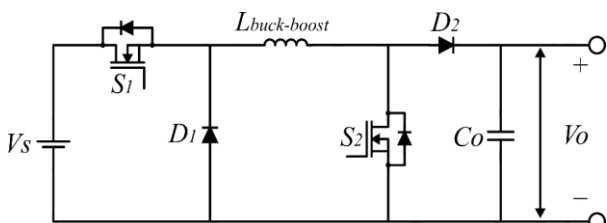


Fig. 1. Two switch non-inverting buck-boost converter

The non-inverting buck-boost converter can operate as a buck, boost and or buck-boost converter depending on the input and output voltage ratio. The two switch, single inductor, non-inverting output topology's buck-boost mode of operation can be implemented in conditions where the input voltage is more, equal, or less than the desired output voltage as depicted in Fig. 2 [22].

The output voltage can be adjusted by controlling the duty cycle of the PWM signals used to control the on and off period of the switches [23]. When the input voltage is higher than the intended output voltage, the buck side switches are more active than the boost side switches; when the input voltage is lower, the boost side switches are more active. During the transition period, when the input and output voltages are equal, both the buck and boost side switches operate equally. The steady-state output voltage has the same magnitude as a traditional buck-boost converter, but it has the same polarity as the input voltage source.

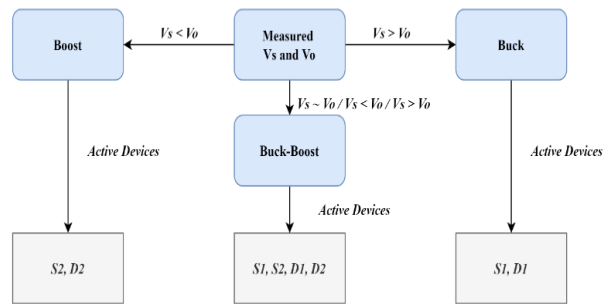


Fig. 2. Operable states of the non-inverting buck-boost converter

In continuous conduction mode (CCM), the converter has two states of operation, mode 1 with the switches  $S1$  and  $S2$  turned on and mode 2 with switches  $S1$  and  $S2$  turned off with a PWM signal of defined frequency and duty cycle. Table II summarizes the mode of operation and corresponding conducting device.

TABLE I  
CONVERTER OPERATIONS MODES

Operation Mode	Switching Devices				Conducting Device
	S1	S2	D1	D2	
Mode 1	1	1	0	0	S1, S2
Mode 2	0	0	1	1	D1, D2

Mode 1 ( $DT_s$ ): In this mode of operation the switches  $S1$  and  $S2$  are turned on whilst storing energy from the input  $V_s$  to the magnetic field of the inductor  $L_{buck-boost}$ , the load is supplied by the output capacitor  $C_o$  in this mode since diode  $D2$  is reversed

biased hence not conducting. The diode  $D1$  is also in a non-conduction state in this mode since it is reverse biased by the input voltage. The equivalent circuit of this mode of operation is depicted in Fig. 3. Eq. 1 and 2 express the inductor voltage and current ripple. Eq. 1 and 2 express the inductor voltage  $V_L$  and current  $\Delta i_L$  with respect to the inductance  $L$ , duty cycle  $D$ , input voltage  $V_s$  and switching period  $T_s$ .

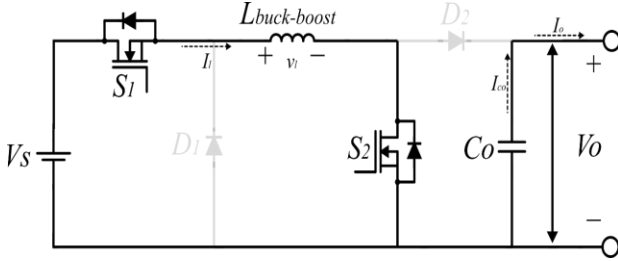


Fig. 3. Equivalent circuit of mode 1 operation

$$v_L = V_s = L \frac{di_L}{dt} \quad (1)$$

$$\Delta i_{L\_closed} = \left(\frac{V_s}{L}\right) DT_s \quad (2)$$

Mode 2( $(1-D) T_s$ ): In this mode of operation the switches  $S1$  and  $S2$  are turned off, and diodes  $D1$  and  $D2$  are forward biased to provide a conduction path for inductor current, hence the stored energy in the magnetic field of inductor supplies the load and charges the output capacitor. The equivalent circuit of this mode of operation is depicted in Fig. 4.

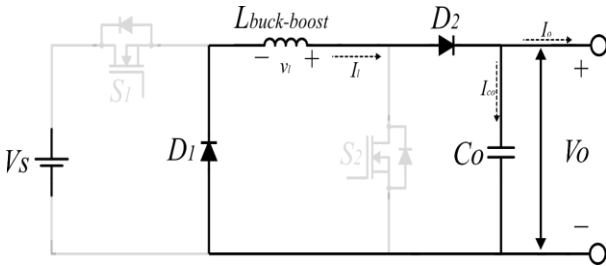


Fig. 4. Equivalent circuit of mode 2 operation

In this mode, inductor voltage  $v_L$  is the same as the output voltages, as represented in Eq. 3 and Eq. 4 expresses the inductor ripple current:

$$v_L = -V_o = L \frac{di_L}{dt} \quad (3)$$

$$\Delta i_{L\_open} = \left(\frac{-V_o}{L}\right) (1-D)T_s \quad (4)$$

Under steady-state operation conditions, the characteristic equations defining the converter operation are given in the series of equations below. The net change in inductor current over a period of

operation should sum up to zero as expressed in Eq. 5.

$$\begin{cases} \Delta i_{L\_closed} + \Delta i_{L\_open} = 0 \\ \left(\frac{V_s}{L}\right) DT_s + \left(\frac{-V_o}{L}\right) (1-D)T_s = 0 \end{cases} \quad (5)$$

The input and output voltage relationships are given in Eq. 6 after simplifying the terms in Eq. 5.

$$V_o = \frac{DV_s}{1-D} \quad (6)$$

The average input power must be equal to the average output power through the load in a steady-state operation as expressed in the equations below.

Average output power:

$$P_o = \frac{V_o^2}{R} = V_o I_o \quad (7)$$

Average input power:

$$V_s I_s = V_s I_L \times D \quad (8)$$

Average input power = Average output power

$$\begin{cases} V_s I_L \times D = \frac{V_o^2}{R} \\ V_s I_L \times D = \frac{V_s^2 D^2}{(1-D)^2 R} \\ I_L = \frac{V_s D}{(1-D)^2 R} \end{cases} \quad (9)$$

The maximum inductor current is simplified in Eq. 10 below.

$$\begin{cases} I_{max} = I_L + \frac{\Delta i_L}{2} \\ I_{max} = \frac{V_s D}{(1-D)^2 R} + \frac{V_s D}{2L f_s} \end{cases} \quad (10)$$

Where:

$$f_s = \frac{1}{T_s} \quad (11)$$

The minimum inductor current is simplified in Eq. 12 below.

$$\begin{cases} I_{min} = I_L - \frac{\Delta i_L}{2} \\ I_{min} = \frac{V_s D}{(1-D)^2 R} - \frac{V_s D}{2L f_s} \end{cases} \quad (12)$$

Eq. 13 expresses the inductance value for a predefined level of current ripple.

$$L = \frac{V_s D}{\Delta i_L f_s} \quad (13)$$

$I_{min}$  must be larger than or equal to zero to continue operating in the continuous conduction mode. This indicates that there is a minimum value of inductance  $L_{min}$  required to operate in this state, which is expressed in Eq. 14.

$$L_{min} = \frac{(1-D)^2 R}{2f_s} \quad (14)$$

Eq. 15 express the relationship between the required output capacitance and the output voltage ripple:

$$\begin{cases} \frac{\Delta V_o}{V_o} = \frac{D}{RCf_s} \\ C = \frac{DV_o}{R\Delta V_o f_s} \end{cases} \quad (15)$$

### III. Control Method

In the closed-loop control of DC-DC converter topologies, several control methods such as sliding mode, fuzzy logic, PI, and model predictive control methodologies are used for the control of output voltage variable to the desired reference value with a relatively good response to variation in system parameters such as input voltage and load variation. To realize a closed-loop control as applied to the non-inverting buck-boost converter topology, the PI, OCC, and Hybrid OCC-PI control methods will be investigated.

#### III.1. PI Control

The PI controller comprises the proportional and integral controllers. The controller improves the response speed and system stability. By comparing the measured and reference values, the error signal is generated which in turn is used to drive the controller to generate the control signal such that the error signal is reduced to nearly zero. The controller reduces the error signal overshoot and takes it to the level of steady-state [7]. Fig. 5 shows the basic configuration of a PI controller. The characteristic response of controller is expressed in Eqs. 16 and 17.

$$v_e(t) = V_{ref}(t) - V_o(t) \quad (16)$$

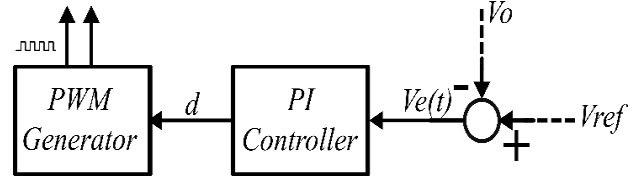


Fig. 5. Conventional PI controller

Where  $v_e(t)$ ,  $V_{ref}(t)$  and  $V_o(t)$  indicate the instantaneous error signal, reference, and output voltages respectively.

$$d(t) = v_e(t) \left( K_p + K_i \frac{1}{s} \right) \quad (17)$$

Where  $d(t)$ ,  $K_p$  and  $K_i$  indicate the instantaneous duty, proportional gain, and integral gains respectively.

#### III.2. OCC Control

The OCC method is also known as the integration-reset technique, and the major component of this control method is the resettable integrator [24]. Observing the switching variables of the buck-boost converter, the output and input voltage relationships show that the output voltage of the converter is the average area of the sum of the input and reference voltages for a given switching period, and thus this methodology can be used to implement a control scheme for a constant frequency control technique [25]. The OCC is a nonlinear control method that consists of a constant frequency clock, comparator and integrator that is used to control the switching signals [26]. In a closed-loop system, the desired output must be equal to the reference value [18]. The mathematical representation of the OCC technique for the non-inverting buck-boost converter can thus be given by the following equations.

$$\begin{cases} V_o = \frac{DV_s}{1-D} \\ V_o = (V_s + V_o)D \end{cases} \quad (18)$$

The steady-state output voltage  $V_o$  is equal to the reference voltage hence:

$$V_{ref} = (V_s + V_{ref})D \quad (19)$$

The average value of the sum of the output voltage and reference voltage over the switching period of the converter is expressed in Eqn. 20 and depicted in Fig. 6.

$$V_{ref} = \frac{1}{T_s} \int_0^{DT_s} (V_s + V_{ref}) dt \quad (20)$$

$$V_{ref}^* = \frac{1}{T_s} \int_0^{DT_s} (V_s + V_{ref}^*) dt \quad (23)$$

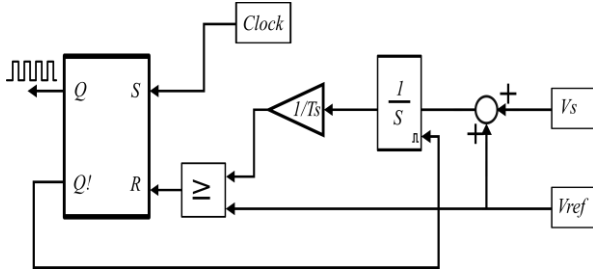


Fig. 6. OCC control of buck-boost converter

### III.3. Hybrid OCC-PI

The Hybrid OCC-PI control method implements an additional PI controller with the conventional OCC control of the buck-boost converter. The controller design of the proposed Hybrid OCC-PI controller is depicted in Fig. 7.

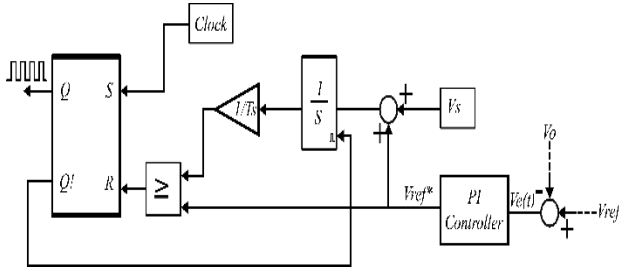


Fig. 7. Hybrid OCC-PI controller for buck-boost converter

The error signal due to the reference and output voltage is used to generate a secondary reference voltage  $V_{ref}^*$  for the internal OCC controller to drive the converter to the desired steady-state reference value. The PI control loop is characterized by Eqs. 21 and 22.

$$v_e(t) = V_{ref}(t) - V_o(t) \quad (21)$$

Where  $V_e(t)$ ,  $V_{ref}(t)$  and  $V_o(t)$  indicate the instantaneous error signal, reference and output voltages respectively.

$$V_{ref}^*(t) = v_e(t) \left( K_p + K_i \frac{1}{s} \right) \quad (22)$$

Where  $V_{ref}^*(t)$ ,  $K_p$  and  $K_i$  indicate the instantaneous secondary reference, proportional and integral gain respectively. The resultant Hybrid OCC-PI controller reference voltage equation is given in Eq. 23.

## IV. Simulation Results

The dynamic response characteristics and performance of the control methods as applied to the buck-boost converter are analyzed using the MATLAB/Simulink simulation environment. The simulation analyses the transient response of the converter for varying load, input voltage and the reference voltage value to observe the converter response for each control method. The converter design parameters for the simulation are summarized in Table II.

A comparison of the simulation results from the PI, OCC and the hybrid OCC-PI control methods is provided in this section. Proportional gains of 0.0001 and 0.00085 are used for the hybrid OCC-PI and conventional PI controls, with integral gains of 350 and 1.5, respectively.

TABLE II  
SIMULATION PARAMETERS

Parameter	Value
Input Voltage, $V_s$	9 – 36 V
Output Voltage, $V_o$	28 V
Output Power, $P_o$	500 W
Output Current, $I_o$	17.86 A
Switching Frequency, $f_s$	250 kHz
Current Ripple	10% of $I_L$
Voltage Ripple	1% of $V_o$
Inductance, $L$	19.82 $\mu$ H
Minimum Inductance, $L_{min}$	0.99 $\mu$ H
Output Capacitor, $C_o$	191.32 $\mu$ F
Duty Cycle Range	43.8 – 75.7%

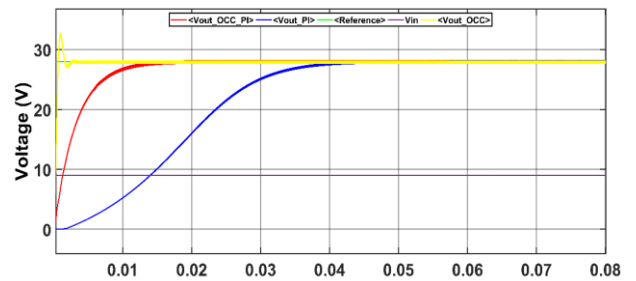


Fig. 8. Converter output voltage response speed for Hybrid OCC-PI and PI control method

Fig. 8 depicts the control response of the converter using the PI, OCC and the hybrid OCC-PI control methods for a constant input voltage  $V_s = 9$  V, the

reference voltage  $V_{ref} = 28$  V, and constant load  $I_O = 17.86$  A. The figure depicts the difference in the converter response speed for each controller under similar operating conditions. Fig. 9 depicts the converter's response to a 3 V step increase in input voltage at a constant reference voltage and load from an input voltage  $V_s = 9$  to 36 V. The simulation results indicate a maximum overshoot of 35.9 %, 12.25% and 13.13 % of the nominal reference voltage for the PI, OCC and hybrid OCC-PI control methods respectively.

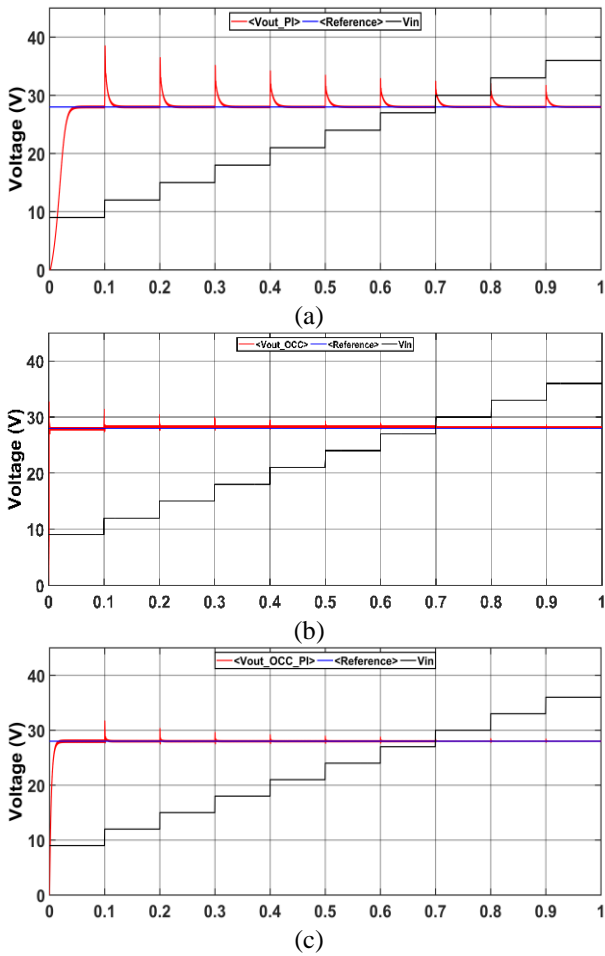


Fig. 9. Output voltage response for input variation: (a) PI control, (b) OCC control, and (c) Hybrid OCC-PI control

The inductor current response observed for an input voltage variation from 9 V to 36 V with an increment of 3 V per step for both control methods are depicted in Fig 10 a. As observed from the simulation results depicted in Fig. 10(a), the inductor current of the PI controlled converter shows a maximum current spike of 40.42% of the nominal inductor current. As observed in Fig. 9(b) and 9(c) however, no inductor current spikes were observed for the OCC and Hybrid OCC-PI control method as applied to the buck-boost converter.

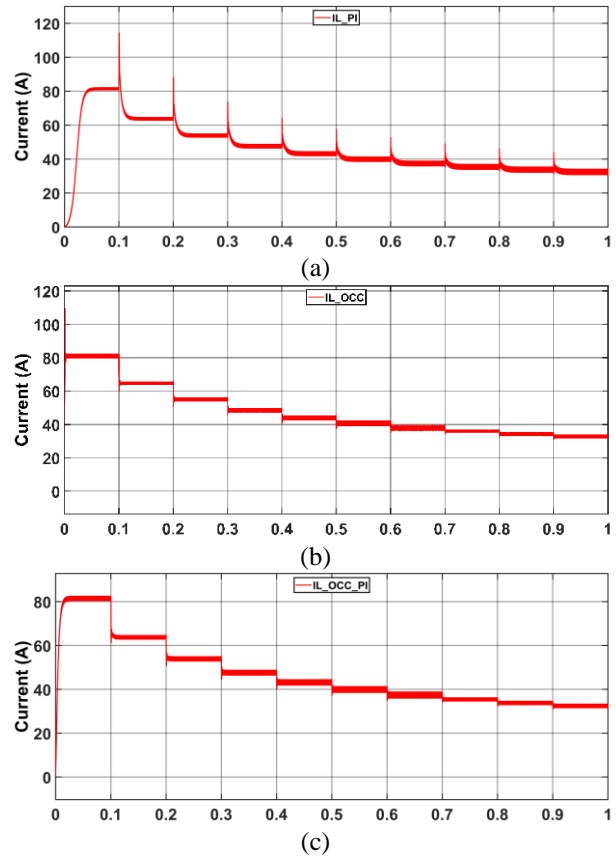


Fig. 10. Output voltage response for input variation: (a) PI control, (b) OCC control, and (c) Hybrid OCC-PI control

The output voltage and inductor current ripple for the control methods are depicted in Fig. 11. During the boost mode of operation, a peak-to-peak voltage ripple of  $0.96 V_{pp}$ ,  $0.28 V_{pp}$  and  $0.97 V_{pp}$  with an inductor current ripple of 1.68 A, 1.68 A and 1.66 A for the PI, OCC and Hybrid OCC-PI control methods respectively were observed. The buck mode operation is characterized by a maximum voltage ripple of  $0.67 V_{pp}$ ,  $0.09 V_{pp}$  and  $0.33 V_{pp}$  with current ripples of 3.23 A, 1.64 A and 1.61 A for the PI, OCC and Hybrid OCC-PI control methods respectively.

Fig. 12 depicts the converter's output voltage for varying reference voltage at a constant switching frequency and input voltage value, the output voltage response is observed. For a nominal voltage of 28 V, the controller's response to a 50% sudden increase in nominal reference voltage and a 50% sudden decrease in nominal reference voltage for the control methods are observed. As depicted in Fig. 12(a) a settling time of 12.41 ms for reference voltage transition from 28 V to 42 V with no voltage overshoot, for a reference voltage transition from 42 V to 14 V a settling time of 44.43 ms and voltage overshoot of 9.05% was observed for the PI controlled buck-boost converter.

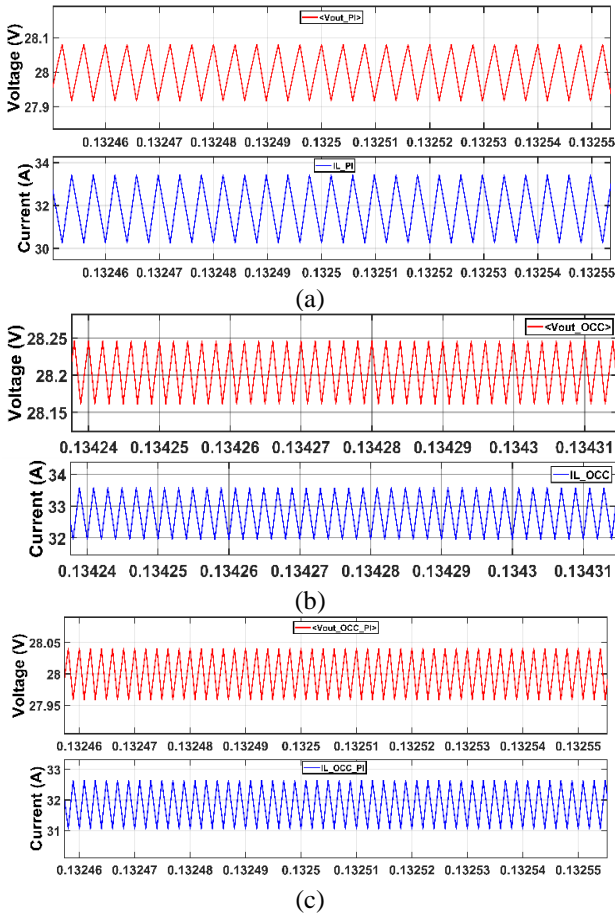


Fig. 11. Output voltage and inductor current ripple: (a) PI control, (b) OCC, and (c) OCC-PI control

Settling time of 2.05 ms with no output voltage overshoot for reference voltage transition from 28 V to 42 was observed for the Hybrid OCC control of buck-boost converter as depicted in Fig. 12(b), for reference voltage transition from 42 V to 14 V a settling time of 2.33 ms and output voltage overshoot of 23.19% was recorded. Settling time of 17.31 ms with no output voltage overshoot for reference voltage transition from 28 V to 42 was observed for the Hybrid OCC-PI control of buck-boost converter as depicted in Fig. 12(c), for reference voltage transition from 42 V to 14 V a settling time of 16.06 ms and output voltage overshoot of 3.98% was recorded.

Fig. 13 depicts the converter's output voltage due to load current variations. The output load response is investigated by varying the system's output load while maintaining a constant switching frequency, reference, and input voltage values. The observed response for an output load variation of +50/-50% of the nominal output current. Settling time and output voltage overshoot of 8.02 ms and 33.74% for load current variation from 17.86 A to 8.93 A and 8.38 ms and -42.51% for load current variation from 8.93 A

to 26.79 A were recorded for the PI controlled buck-boost converter, as shown in Fig. 13(a).

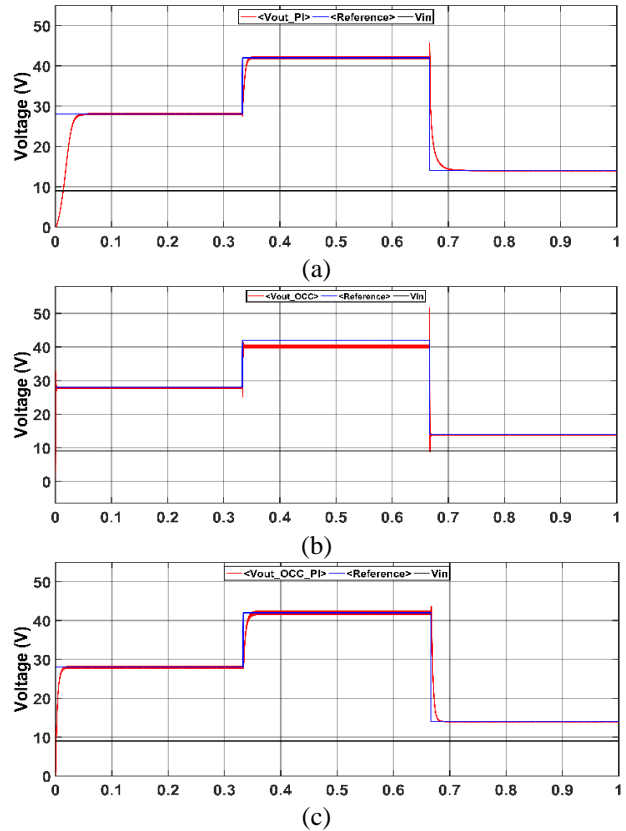


Fig. 12. Output voltage response for varying reference voltage: (a) PI control, (b) OCC, and (c) Hybrid OCC-PI control

Settling time and output voltage overshoot of 3.68 ms and 33.93% for load current variation from 17.86 A to 8.93 A and 1.84 ms and -40.29% for load current variation from 8.93 A to 26.79 A were recorded for the PI controlled buck-boost converter, as shown in Fig. 13(a). It is also observed that the output voltage deviates from the reference value. For lower load the output voltage increases by 1.42 V and for higher loads the voltage drops by 1.36 V from the reference value. As shown in Fig. 13(c), the Hybrid OCC-PI controlled buck-boost converter had a settling time of 5.74 ms and an output voltage overshoot of 34.27% for a load current variation of 17.86 A to 8.93 A, and a settling time of 3.85 ms and an output voltage overshoot of -42.45% for a load current variation of 8.93 A to 26.79 A.

Table III summarizes the simulation results' observed performance characteristics, such as output voltage ( $V_o$ ), settling time ( $T_{ST}$ ), percentage output voltage overshoots ( $V_{OS}$ ), output voltage ripple ( $\Delta V_o$ ), inductor current ripple ( $\Delta I_L$ ) and the efficiency ( $\eta$ ) of the converter for different operation conditions utilizing the two control methods.

TABLE III  
 CONTROLLER RESPONSE CHARACTERISTICS

Conditions		Control Method																	
		PI Control						OCC Control					Hybrid OCC-PI Control						
		Vo (avg)	V <sub>OS</sub> (%)	Δv <sub>i</sub> (V <sub>pp</sub> )	Δi <sub>i</sub> (A)	T <sub>ST</sub> (ms)	η%	Vo (avg)	V <sub>OS</sub> (%)	Δv <sub>i</sub> (V <sub>pp</sub> )	Δi <sub>i</sub> (A)	T <sub>ST</sub> (ms)	η%	Vo (avg)	V <sub>OS</sub> (%)	Δv <sub>i</sub> (V <sub>pp</sub> )	Δi <sub>i</sub> (A)	T <sub>ST</sub> (ms)	η%
V <sub>s</sub> Variation	9 – 12 V	28.00	35.97	0.96	1.68	24.87	91.41	28.26	12.25	0.28	1.68	2.24	90.84	28.00	13.13	0.97	1.66	4.15	91.02
	12 – 15 V	28.00	28.64	0.89	1.98	21.32	92.85	28.33	8.82	0.26	2.04	1.91	92.49	28.00	8.25	0.89	1.97	1.98	92.67
	15 – 18 V	28.00	23.82	0.83	2.22	20.01	93.76	28.35	6.64	0.24	2.27	1.73	93.33	28.00	5.72	0.84	2.23	1.66	93.65
	18 – 21 V	28.00	20.48	0.78	2.47	19.12	94.39	28.32	5.25	0.23	2.51	1.52	94.13	28.00	4.21	0.78	2.42	1.41	94.28
	21 – 24 V	28.00	17.91	0.74	2.68	18.1	94.7	28.29	4.32	0.21	2.63	1.39	94.64	28.00	3.26	0.73	2.63	1.32	94.64
	24 – 27 V	28.00	15.92	0.7	2.84	17.97	94.96	28.28	3.61	0.2	2.82	1.23	94.73	28.00	2.64	0.7	2.82	1.21	94.91
	27 – 30 V	28.00	14.18	0.67	3.01	17.2	95.18	28.25	2.25	0.1	1.51	1.23	95.11	28.00	1.42	0.33	1.49	1.12	95.15
	30 – 33 V	28.00	12.77	0.63	3.18	16.53	95.34	28.22	2.43	0.09	1.59	1.14	95.23	28.00	1.65	0.31	1.63	1.1	95.23
	33 – 36 V	28.00	11.68	0.61	3.23	15.05	95.51	28.2	2.11	0.09	1.64	1.06	95.42	28.00	1.38	0.3	1.61	1.03	95.44
V <sub>ref</sub> Variation	28 V	28.00	-	1.04	1.31	45.63	87.58	27.92	17.2	0.44	1.96	2.29	88.32	28.00	-	1.54	1.96	15.1	87.83
	42 V	42.00	-	1.14	1.27	12.41	77.95	41.45	-	0.94	2.58	2.05	79.21	42.00	-	2.29	2.53	17.31	78.11
	14 V	14.00	9.05	0.84	1.12	44.43	90.84	13.75	23.19	1.17	1.13	2.33	90.97	14.00	3.98	0.84	1.12	16.06	90.73
I <sub>o</sub> Variation	17.86 A	28.00	-	1.04	1.31	45.63	87.58	27.92	17.2	0.44	1.96	2.29	88.32	28.00	-	1.54	1.96	15.1	87.83
	8.93 A	28.00	33.74	0.51	1.27	8.02	92.44	29.42	33.93	2.31	2.09	3.68	93.54	28.00	34.27	0.77	2.02	5.74	92.38
	26.79 A	28.00	-42.51	1.55	1.35	8.38	82.25	26.64	-40.29	0.62	1.91	1.84	84.11	28.00	-42.45	2.31	1.91	3.85	82.46
Nominal	28 V/17.86 A	28.00	-	1.04	1.31	45.63	87.58	27.92	17.2	0.44	1.96	2.29	88.32	28.00	-	1.54	1.96	15.1	87.83

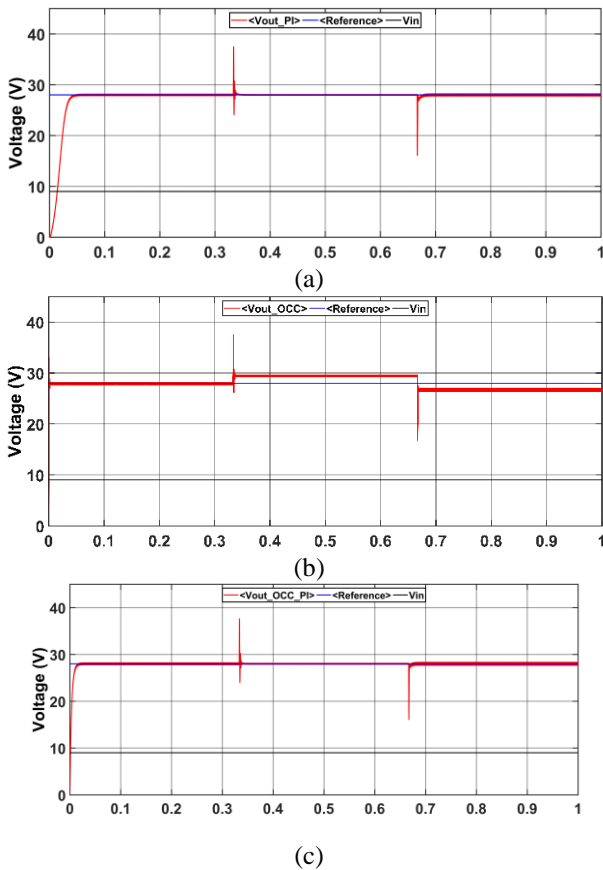


Fig. 13. Output voltage response for a varying load: (a) PI control, (b) OCC, and (c) Hybrid OCC-PI control

## V. Conclusion

Using an equivalent MATLAB/Simulink model, the paper compares the performance of the PI, OCC and the Hybrid OCC-PI controlled buck-boost converter. For varying operating conditions of input

voltage, reference voltage, and load current variations, the simulation results show consistency with the theoretical values, and the observed characteristic response of the converter is shown in Table 3. The response characteristic of each control method as shown in Table 3 indicates that the Hybrid OCC-PI control method provides a relatively faster settling time than the PI control method and relatively less overshoot than the OCC control method. Under all conditions of operation, the maximum settling times were 3.68 ms, 16.06 ms and 45.63 ms for the OCC, Hybrid OCC-PI and PI control methods respectively. Under all operating conditions, the maximum output voltage overshoots for the OCC, Hybrid OCC-PI and PI control methods were 33.93%, 34.27% and 35.97%, respectively, with minimum values of 2.11%, 1.38% and 9.05%. Because the input voltage is included in the control loop, the OCC and Hybrid OCC-PI control method provides a relatively better performance in terms of output voltage overshoot due to input voltage variations. Typical maximum efficiencies of 95.42%, 95.44% and 95.51% were recorded for the OCC, Hybrid OCC-PI and PI controlled buck-boost converters respectively for an input voltage of 36 volts and a reference voltage of 28 volts. Minimum efficiencies of 79.21%, 78.11% and 77.95% for the OCC, Hybrid OCC-PI and PI control methods, respectively, for a reference voltage of 42 volts and an input voltage of 9 volts. The PI control method provides relatively lower output voltage ripple as compared to the Hybrid OCC-PI control method with maximum voltage ripple of 2.31 V<sub>pp</sub>, 2.31 V<sub>pp</sub> and 1.31 V<sub>pp</sub> for the OCC hybrid OCC-PI and PI control methods respectively. Although the OCC

control provides faster response to a variation of the parameters however it was observed that for the OCC controlled converter the output voltage does not effectively track the reference value due to the absence of the output voltage in the control loop as depicted in Fig 13 (b). The hybrid OCC-PI control method provide a relatively faster response than the PI control with lower output voltage overshoots. Due to the inclusion of the output voltage in the control loop the hybrid OCC-PI provides better tracking of the reference voltage. Hence, it can be concluded from the simulations results that the Hybrid OCC-PI control method provides relatively better performance than the other control methods as applied to the non-inverting buck boost converter.

### References

- [1] Z. Ortatepe and A. Karaarslan, "Pre-calculated duty cycle optimization method based on genetic algorithm implemented in DSP for a non-inverting buck-boost converter", *J Power Electron*, 20(1), 34–42, 2020. DOI: <https://doi.org/10.1007/s43236-019-00009-2>
- [2] S. Singh, B. Singh, G. Bhuvaneswari, V. Bist, A. Chandra, and K. Al-Haddad, "Improved power quality bridgeless converter based multiple output SMPS", *IEEE Trans Ind Appl*, 51(1), 721–32, 2015.
- [3] S. Singh, B. Singh, G. Bhuvaneswari, and V. Bist, "Improved Power Quality Switched-Mode Power Supply Using Buck-Boost Converter". *IEEE Trans Ind Appl*. 52(6), 5194–202, 2016.
- [4] C. Chang, and C. Chen, "An isolated output-feedback scheme with minimized standby power for SMPS". *IEEE Trans Power Electron*, 28(11), 5140–5146, 2013.
- [5] A. Ghosh, and S. Saran, "High gain DC-DC step-up converter with multilevel output voltage". *2018 Int. Symp. Devices, Circuits Syst ISDCS 2018*, pp. 1–6. 2018.
- [6] H. Gholizadeh, N. Totonchi, R. Shahrivar, S. Mahdizadeh, E. Afjei, and A. Abbasi, "Design and implementation of a transformerless high step-up dc-dc converter based on conventional boost converter and voltage multiplier cells". *12th Power Electron Drive Syst Technol Conf (PEDSTC)*. 2021.
- [7] A. Farzin, P. Sawai, E. Kei, L. Ngo, C. Dorf, "Modeling uncertainties in DC-DC converters with MATLAB and PLECS", *Morgan & Claypool*. 2018.
- [8] M. A. Sakka, J. V. Mierlo, H. Gualous, "DC/DC converters for electric vehicles", *Electric Vehicles - Modelling and Simulations*. London, United Kingdom: IntechOpen, 2011, DOI: 10.5772/17048
- [9] J. M. Galm, "Analysis and Opinion on the Operation of Switch Mode Power Supplies under Switched Voltage Phase Conditions", *LayerZero Power Systems, Inc.*, pp. 1–8. 2003.
- [10] E. Serri, and A. Ahmad, "Comparative study of short prediction MPC-KF with PI controller for DC-DC buck converter", *Proc - 2016 IEEE Int. Conf. Autom. Control Intell. Syst. I2CACIS*. 219–224. 2016.
- [11] M. Alarabi, and A. Karaarslan, "The design of isolated multiphase interleaved converter for battery charging of military applications", *SN Appl. Sci.*, 2(3), 1–7. 2020.
- [12] A. Karaarslan, "Hysterisis control of power factor correction with a new approach of sampling technique". *IEEE Conv. Electr. Electron Eng. Isr. Proc.*, 765–769. 2008.
- [13] Z. Ortatepe, and A. Karaarslan, "The performance analysis of AC-DC bridgeless converter using fuzzy self-tuning and comparing with PI control method", *J. Intell. Fuzzy Syst.* 35(4), 4629–4642. 2018.
- [14] Z. Ortatepe, and A. Karaarslan, "Error minimization based on multi-objective finite control set model predictive control for matrix converter in DFIG", *Int. J. Electr. Power Energy Syst.* 126(PA) 106575, 1-10. 2021.
- [15] A. Karaarslan, "Modeling and performance analysis of cuk converter using PI and OCC method". *Int. J. Technical Phys. Probl. Eng.*, 10(3), 1–5. 2018.
- [16] O. Ozkara, N. Tokgoz, R. Dogan, and A. Karaarslan "The Analysis of OCC and PI Control Method for Isolated Fly-Back Converter using PEM Fuel Cells", *Gaziosmanpasa Journal of Scientific Research*, 6, 40–49. 2017.
- [17] A. Karaarslan, "The implementation of one cycle control method to inverting buck-boost converter", *Int. J. "Technical Phys. Probl. Eng.*, 10(2), 14-19. 2018.
- [18] M. Bildirici, and A. Karaarslan, "Analysis of Cuk Converter Using Pi and OCC Control Method", *13th Int. Conf. Technical Phys. Probl. Eng.*, Van Turkey, 144-148. 2017.
- [19] M. Z. Erel, M. Ozev, and A. Karaarslan, "The comparison of OCC and PI control method for DC-DC boost converter", *8th International Advanced Technologies Symposium*, Elazığ, Turkey, 3213 – 3220. 2017.
- [20] E. Bektaş, and A. Karaarslan, "The comparison of PI control method and one cycle control method for SEPIC converter". *10th Int. Conf. Electr. Electron Eng. (ELECO 17)*, Bursa, Turkey, pp. 345-349. 2017.
- [21] Z. Uysal, and A. Karaarslan, "Comparison of one cycle and PI control method using Buck-boost converter". *Proc. 13th Int Conf Tech Phys Probl Electr Eng.*, 115–20. 2017.
- [22] V. Choudhary, H. Timothy, and P. David, "Under the hood of a noninverting buck-boost converter", *Power Supply Design Seminar*, 23. 2016.
- [23] R. Keskin, and I. Aliskan, I., "Design of non-inverting buck-boost converter for electronic ballast compatible with led drivers", *Karaelmas Science Engineering Journal*, 8(2), pp. 473–481. 2018.

- [24] K. Bolor, and N. Halvaei, “Implementation of a novel brushless DC motor drive based on one-cycle control strategy”, *5th Annu. Int. Power Electron Drive Syst. Technol. Conf.* pp. 55–60. 2014.
- [25] S. Čuk, “One-cycle control of switching converters”. *IEEE Trans Power Electron.*, 10(6), 625–33. 1995.
- [26] E. Şeker, M. Benli, and A. Karaarslan, “The analysis of one cycle control method using DC-DC isolated forward converter”. *8th International Advanced Technologies Symposium*, Elazığ, Turkey, pp. 3582-3589. 2017.

### Authors’ information



**Ahmet Karaarslan** received the M.Sc. and PhD degrees in Electrical and Electronics Engineering from Gazi University, Ankara, Turkey, in 2005 and 2011, respectively. He is currently an Associated Professor with the Faculty of Engineering and Natural Sciences at Yildirim Beyazit University, Ankara, Turkey. His research interests are in the

application of circuits of power electronics, energy conversion systems, programming microprocessors, renewable energy sources, electrical machines, and computer applications.



**Ali Shaibu** received the BSc and MSc degrees in Electrical and Electronics Engineering from the University of Mines and Technology, Tarkwa and Ankara Yildirim Beyazit University Turkey, in 2016 and 2022 respectively. He was a research associate at the AYBU Power Electronics Laboratory. His research interests include power electronic techniques, renewable

energy, energy conversion and control.